CAMBRIDGE

Cambridge University Press
978-1-107-01898-3 - The Weather and Climate: Emergent Laws and Multifractal Cascades
Shaun Lovejoy and Daniel Schertzer
Excerpt
More information

Chapter 1

Introduction

1.1 A new synthesis

1.1.1 Two (irreconcilable?) approaches to understanding the atmosphere

In the last 20 years there has been a quiet revolution in atmospheric modelling. It's not just that computers and numerical algorithms have continued their rapid development, but rather that the very goal of the modelling has profoundly changed. Whereas 20 years ago, the goal was to determine the (supposedly) unique state of the atmosphere, today with the advent in Ensemble Forecasting Systems (EFS), the aim is to determine the possible future atmospheric states including their relative probabilities of occurrence: this new goal is *stochastic*. A *stochastic process* is a set of random variables indexed by time (Kolmogorov, 1933), and this definition includes that of deterministic processes as a special case.

At present, the EFS are really hybrids in the sense that they operate by first generating an initial ensemble of atmospheric states compatible with the observations and then use conventional deterministic forecasting techniques to advance each member in time to produce a distribution of future states. Once the leap was taken to go beyond the forecasting of a unique state to forecasting an ensemble, the next step was to make the subgrid parametrizations themselves stochastic (e.g. Buizza *et al.*, 1999; Palmer, 2001; Palmer and Williams, 2010). This is an attempt to take into account the variability of different possible subgrid circulations. The artificial deterministic/stochastic nature of these hybrids suggests that the development or pure stochastic forecasts would be advantageous, a possibility we explore in Chapter 9.

Interestingly, the tension between determinism and stochasticity has been around pretty much since the beginning, although for most of the (still brief) history of atmospheric science the deterministic approaches have been in the ascendancy and the stochastic ones left in the wings. To see this, let us recall the important developments. Drawing on the classical (deterministic) laws of fluid mechanics, Bjerknes (1904) and Richardson (1922) extended these to the atmosphere in the now familiar form of a closed set of nonlinear partial differential governing equations. From a mathematical point of view, their deterministic character is evident from the absence of probability spaces; from a conceptual point of view, it is associated with classical Newtonian thinking. In physics, Newtonian determinism began to disappear with the advent of statistical mechanics (starting with the "Maxwellian" distribution of molecular velocities: Maxwell, 1890), which showed that physical theories could indeed be stochastic. The break with determinism was consecrated with the development of quantum mechanics, which is a fundamental yet stochastic theory where the key physical variable – the wavefunction – determines probabilities.

At roughly the same time as the basis of modern deterministic numerical weather prediction was being laid, an alternative stochastic "turbulent" approach was being developed by G. I. Taylor, L. F. Richardson, A. N. Kolmogorov and others. Just as in statistical mechanics, where huge numbers of degrees of freedom exist but where only certain "emergent" macroscopic qualities (temperature, pressure etc.) are of interest, in the corresponding turbulent systems the new theories sought to discover new emergent statistical turbulence laws.

The first of these emergent turbulent laws was the Richardson "4/3 law" of atmospheric diffusion: $\nu(L) \approx KL^{4/3}$, where $\nu(L)$ is the effective viscosity at scale L and K is a constant to which we return (Richardson, 1926): see Fig. 1.1. This law is famous not only as the precursor of the Kolmogorov (1941) law of 3D isotropic homogeneous turbulence (the "5/3" law for the spectrum – or, if expressed for the fluctuation $\Delta v(L)$, the "1/3" law: $\Delta v(L) = \varepsilon^{1/3}L^{1/3}$ where Δv is the velocity fluctuation and ε is the energy flux), but it is also celebrated thanks to the

© in this web service Cambridge University Press www.cambridge.org

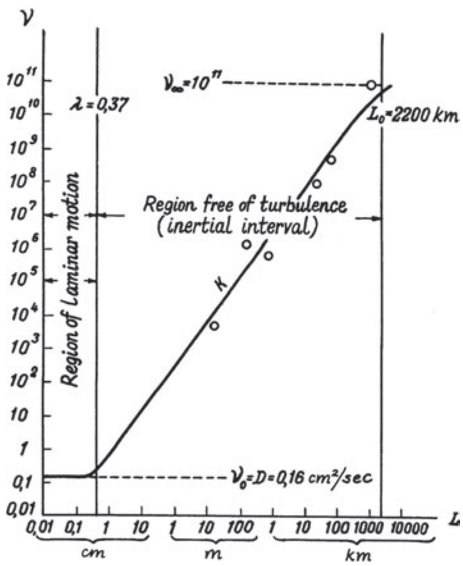

Fig. 1.1 Effective viscosity as a function of scale, reproduced from Monin (1972), adapted from (Richardson, 1926). The text (inserted by Monin) should read "region of free turbulence"(!)

ingenious way that Richardson experimentally confirmed his theory with the help of balloons and later even with parsnips and thistledown (Richardson and Stommel, 1948)! While this attention is all well deserved, the law was perhaps even more remarkable for something else: that Richardson had the audacity to conceive that a unique scaling (power) law – i.e. a law without characteristic length scales – could operate over the range from millimetres to thousands of kilometres, i.e. over essentially the entire meteorologically significant range. In accord with this, Richardson believed that the corresponding diffusing particles had "Weierstrass function-like" (i.e. fractal) trajectories. Nor was the 4/3 law an isolated result. In the very same pioneering book, *Weather Prediction by Numerical Process* (Richardson, 1922), in which he wrote down essentially the modern equations of the atmosphere (Lynch, 2006) and even attempted a manual integration, he slyly inserted:

> Big whirls have little whirls that feed on their velocity,
> and little whirls have lesser whirls and so on to
> viscosity – in the molecular sense.

Thanks to this now iconic poem, Richardson is often considered the grandfather of the modern cascade theories that we discuss at length in this book.

Had Richardson been encumbered by later notions of the meso-scale – or of isotropic turbulence in either two or three dimensions – he might never have discovered his law. Already, 15 years after he proposed it, Kolmogorov (1941) humbly claimed only a relatively small range of validity of the stringent "inertial range" assumptions of statistical isotropy and homogeneity which he believed were required for the operation of his eponymous law (which was also discovered, apparently independently, by Obukhov, 1941b, 1941a; Onsager 1945; Heisenberg, 1948; and von Weizacker, 1948) – and this even though it has strong common roots with Richardson's law. Indeed, it implies that Richardson's proportionality constant depends on the energy flux ε: $\nu(L) = L\Delta v(L) = \varepsilon^{1/3}L^{4/3}$; in this sense Kolmogorov's contribution was to find $K = \varepsilon^{1/3}$. Echoing Kolmogorov's reservations, Batchelor (1953) speculated that the Kolmogorov law should only hold in the atmosphere over the range 100 m to 0.2 cm! Even in Monin's influential book *Weather Forecasting as a Problem in Physics* (1972), the contradiction between the small and wide ranges of validity of the Kolmogorov and Richardson 4/3 laws is pushed surprisingly far, since on the one hand Monin confines the range of validity of the $\Delta v(L) = \varepsilon^{1/3}L^{1/3}$ law to "micrometerological oscillations ... up to ≈ 600 m in extent," while on the other hand publishing (on the opposite page!) a reworked copy of Richardson's figure demonstrating the validity of the $\nu(L) \approx L^{4/3}$ up to thousands of kilometres (Fig. 1.1). For the latter, he comments that it "is valid for nearly the entire spectrum of scales of atmospheric motion from millimeters to thousands of kilometres," in accord with Richardson. In Monin and Yaglom (1975), the contradiction is noted with the following mysterious explanation: "in the high frequency region one finds unexpectedly, that relationships similar to those valid in the inertial subrange of the microturbulence spectrum are again valid." In Chapter 6 we argue on the basis of modern reanalyses and other data that the law $\Delta v(L) = \varepsilon^{1/3}L^{1/3}$ does indeed hold up to near planetary scales in the horizontal, but paradoxically that, even at scales as small as 5 m, it does *not* hold in the vertical (and hence 3D isotropic turbulence does not seem to hold anywhere in the atmosphere)! By proposing a theory of anisotropic but scaling turbulence, we attempt to explain how it is possible that Kolmogorov was simultaneously *both* so much *more* accurate (the horizontal) and yet so much *less* accurate (the vertical) than anyone expected. This was achieved with the help of a generalized notion of scaling (Schertzer and Lovejoy, 1985a, 1985b) which ironically led to an effective "in between" dimension of atmospheric turbulence $D = 23/9 = 2.55...$ and enables the Fractal Geometry

© in this web service Cambridge University Press www.cambridge.org

CAMBRIDGE

Cambridge University Press
978-1-107-01898-3 - The Weather and Climate: Emergent Laws and Multifractal Cascades
Shaun Lovejoy and Daniel Schertzer
Excerpt
More information

to at last (!) escape from the Euclidean metric (Schertzer and Lovejoy, 2006).

Facing colossal mathematical difficulties, turbulence theorists, starting with Taylor (1935), concentrated their attentions on the simplest turbulence paradigm: turbulence that is statistically isotropic, first in 3D, and then – following Fjortoft (1953) and Kraichnan (1967) – on the special isotropic 2D case. While Charney did extend Kraichnan's 2D theory to the atmosphere in his seminal paper "Geostrophic turbulence" (1971), meteorologists had already begun focusing on numerical modelling. By the end of the 1970s, there had thus developed a wide divergence between, on the one hand, the turbulence community with its focus on statistical closures and statistical models of intermittency (especially cascades) and, on the other hand, the meteorology community with its focus on practical forecasting and which treated turbulence primarily as a subgrid parametrization problem.

1.1.2 Which chaos for geophysics, for atmospheric science: deterministic or stochastic?

The divergence between statistical and deterministic approaches was brought into sharp relief thanks to advances in the study of nonlinear systems with few degrees of freedom. The new science of "deterministic chaos" can be traced back to the pioneering paper "Deterministic nonperiodic flow" (Lorenz, 1963) (and has antecedents in Poincaré, 1892). Lorenz's 1963 paper caused excitement by showing that three degrees of freedom were sufficient to generate chaotic (random-like) behaviour in a purely deterministic system. At the time, it was widely believed (following Landau, 1944) that on the contrary, random-like behaviour was a consequence of a very large number of degrees of freedom, so that as the nonlinearity increased (e.g. the Reynolds number) a fluid became fully turbulent only after successively going through a very large (even infinite) number of instabilities. By showing that as few as three degrees of freedom were necessary for chaotic behaviour, Lorenz's paper opened the door to the possibility that turbulence could have a relatively low-dimensional "strange attractor" so that effectively only a few degrees of freedom might matter. However, Lorenz's observation did not immediately lead to practical applications because theorists can readily invent nonlinear models, and at the same time it appeared that each model would require its own in-depth study in order to understand its behaviour. The problem of apparent lack of commonality in different nonlinear systems is the now familiar problem of "universality" which Fischer, Kadanoff and Wilson were only then successfully understanding and exploiting in the physics of critical phenomena; we shall revisit universality later in this book (Chapter 3). It is therefore not surprising that the turning point for deterministic chaos was precisely the discovery of "metric" (i.e. quantitative) "universality" by Grossman and Thomae (1977) and Feigenbaum (1978): the famous Feigenbaum constant in period doubling maps. Soon, with the help of theorems such as the extension of the Whitney embedding theorem (Whitney, 1936) and the practical "Grassberger–Procaccia algorithm" (Grassberger and Procaccia, 1983a, 1983b), all manner of time series were subjected to nonlinear analysis in the hope of "reconstructing the attractor" and of determining its dimension, which was interpreted as an upper bound on the number of degrees of freedom needed to reproduce the system's behaviour. In fact – as argued by Schertzer *et al.* (2002), Schertzer and Lovejoy (2003) – the mathematics do not support such a statement: they showed that indeed a stochastic cascade process may yield a finite correlation dimension, whereas the process itself has an infinite dimension! They therefore raised the question "which chaos?" For climate models essentially the same question was asked by Lorenz (1975), and more recently Palmer (2012) has strongly defended stochastic approaches.

Other developments in the 1980s helped to transform the "deterministic chaos revolution" into a more general "nonlinear revolution." Of particular importance for this book was the idea that many geosystems were fractal (scale invariant) (Mandelbrot, 1977, 1983) and later, that they commonly displayed "self-organized criticality" (SOC) (Bak *et al.*, 1987; Bak, 1996), implying that many real-world systems could be "avalanche-like." Indeed, SOC is so extreme that even "typical" structures are determined by extreme events (see Chapter 5 for the connection between SOC and turbulent cascades).

The success of the apparently opposed paradigms of deterministic chaos and (stochastic) fractal systems thus sharply posed the question "which chaos for atmospheric science: deterministic or stochastic?" The question was not the philosophical one of

© in this web service Cambridge University Press www.cambridge.org

Cambridge University Press
978-1-107-01898-3 - The Weather and Climate: Emergent Laws and Multifractal Cascades
Shaun Lovejoy and Daniel Schertzer
Excerpt
More information

whether or not the world is deterministic or stochastic, but rather whether deterministic or stochastic models are the most fruitful: which is the closest to reality (Lovejoy and Schertzer, 1998)? The answer to this question essentially depends on the number of degrees of freedom that are important: since stochastic systems are usually defined on infinite dimensional probability spaces they are good approximations to systems with large numbers of degrees of freedom. As applied to the atmosphere, the classical estimate of that number is essentially the number of dissipation scale fluid elements in the atmosphere, roughly 10^{27}–10^{30} (see Chapter 2 for this estimate). However, at any given moment clearly many of these degrees of freedom are inactive, and indeed we shall see that multifractals (via the codimension function $c(\gamma)$, Chapter 5) provide a precise estimate of the fraction of those at any given level of activity and at any space-time scale.

1.2 The Golden Age, revolution resolution and paradox: an up-to-date empirical tour of atmospheric variability

1.2.1 The basic form of the emergent laws and spectral analysis

Without further mathematical or physical restrictions, the high number of degrees of freedom paradigm of stochastic chaos is too general to be practical. But with the help of a scale-invariant symmetry such that in some generalized sense the dynamics repeat scale after scale, it becomes tractable and even seductive. It turns out that the equations of the atmosphere are indeed formally scale-invariant (Chapter 2), and even fields for which no theoretically “clean” equations exist (such as for precipitation) still apparently respect such scale symmetries. However, even if the equations respect a scaling symmetry, the solutions (i.e. the real atmospheric motions) would not be scaling were it not for the scale invariance of the relevant boundary conditions.

We have briefly mentioned the Kolmogorov law as being an example of an emergent law. Indeed, all the emergent laws discussed in this book are of the form:

$$\boxed{\mathit{Fluctuations} \approx (\mathit{turbulent\ flux})^a \times (\mathit{scale})^H \quad (1.1)}$$

The Kolmogorov law mentioned in the previous section is recovered as a special case if the velocity difference Δv across a fluid structure of a given scale (L) is used for the fluctuations and we take the scaling exponent $H = 1/3$ and the turbulent flux is ε and $a = 1/3$. The book is structured around a series of generalizations of this basic equation. For example, rather than considering smooth or weakly varying (for example quasi-Gaussian) fluxes, we show in Chapters 3 and 5 how to treat wildly variable fluxes that are the results of multiplicative (and multifractal) cascades (this involves interpreting the equality in Eqn. (1.1) in the sense of random variables). Then in Chapters 6 and 7 we generalize the notion of “scale” to include strong anisotropy – needed in particular for handling atmospheric stratification (“generalized scale invariance”). In Chapters 8 and 9 this is further generalized from anisotropic space to anisotropic space-time (including causality). Finally in Chapter 10 we show how the long-time behaviours of space-time cascades involve “dimensional transitions” and low-frequency weather fluctuations with $H < 0$. According to Eqn. (1.1), since the mean of the turbulent flux is independent of scale this “macroweather” regime is characterized by mean fluctuations that decrease with scale. This contrasts with the higher-frequency “weather” regime in which typically $H > 0$ so that, on the contrary, mean weather fluctuations increase with scale. Box 1.1 (below) discusses the typical types of variability associated with different H values.

We now proceed to give an empirical tour of some of the fields relevant either directly or indirectly to atmospheric dynamics. This overview is not exhaustive, and it partly reflects the availability of relevant analyses and partly the significance of the fields in question. Our aim is to exploit the current “golden age” of geophysical observations so as to demonstrate as simply as possible the ubiquity of wide-range scaling – even up to planetary scales – and hence the fundamental relevance of scaling symmetries for understanding the atmosphere. However, before setting out to empirically test Eqn. (1.1) on atmospheric fields, a word about fluctuations. Often, the definition of a fluctuation as simply a difference is adequate (strictly speaking when $0 < H < 1$), but sometimes other definitions are needed. Indeed, there has arisen an entire field – wavelets – centred essentially around systematic ways of defining and handling fluctuations. For most of the following, thinking of fluctuations as differences is adequate, but some mathematical formalism is developed in Section 5.5, and as a practical matter, differences are

© in this web service Cambridge University Press www.cambridge.org

CAMBRIDGE

Cambridge University Press
978-1-107-01898-3 - The Weather and Climate: Emergent Laws and Multifractal Cascades
Shaun Lovejoy and Daniel Schertzer
Excerpt
More information

not adequate in Chapter 10, where we treat macroweather which has $H < 0$ and requires other definitions of fluctuations (we recommend the simple Haar fluctuation, but others are possible).

In the following scaling overview, it will therefore be convenient to use the Fourier (spectral) domain version of Eqn. (1.1), which avoids these technical issues. In Fourier space, Eqn. (1.1) reads:

$$\left(\frac{Variance_{observables}}{wavenumber}\right) = \left(\frac{Variance_{flux^a}}{wavenumber}\right)(wavenumber)^{-2H} \tag{1.2}$$

Consider a random field $f(\underline{r})$ where $\underline{r}$ is a position vector. Its "variance/wavenumber" or "spectral density" $E(k)$ is the total contribution to the variance of the process due to structures with wavenumber between k and $k + dk$, i.e. due to structures of size $l = 2\pi/k$ where l is the corresponding spatial scale and $k = |\underline{k}|$ (the modulus of the wavevector); we postpone a more formal definition to Chapter 2. The spectral density thus satisfies:

$$\langle f(\underline{r})^2\rangle = \int_0^\infty E(k)dk \tag{1.3}$$

where $\langle f(\underline{r})^2\rangle$ is the total variance (assumed to be independent of position; the angular brackets "<·>" indicate statistical averaging).

In the following examples we demonstrate the ubiquity of power law spectra:

$$E(k) \approx k^{-\beta} \tag{1.4}$$

If we now consider the real space (isotropic) reduction in scale by factor λ we obtain: $\underline{r} \rightarrow \lambda^{-1}\underline{r}$ corresponding to a "blow up" in wavenumbers: $k \rightarrow \lambda k$; power law spectra $E(k)$ (Eqn. (1.4)) maintain their form under this transformation: $E \rightarrow \lambda^{-\beta}E$ so that E is "scaling" and the (absolute) "spectral slope" β is "scale-invariant." If empirically we find E of the form Eqn. (1.4), we take this as evidence for the scaling of the field f. For the moment, we consider only scaling and scale invariance under such conventional isotropic scale changes; in Chapter 6 we extend this to anisotropic scale changes.

1.2.2 Atmospheric data in a Golden Age

As little as 25 years ago, few atmospheric datasets spanned more than two orders of magnitude in scale; yet they were challenging even to visualize. Global models had even lower resolutions, yet required heroic computer efforts. The atmosphere was seen through a low-resolution lens. Today, in-situ and remote data routinely span scale ratios of 10^3–10^4 in space and/or time scales, and operational models are not far behind. We are now beginning to perceive the true complexity of atmospheric fields which span ratios of over 10^{10} in spatial scales (the planet scale to the dissipation scale). One of the difficulties in establishing the statistical properties of atmospheric fields is that it is impossible to estimate spatial fields without making important assumptions about their statistical properties. We now survey the main data types, indicating some of their limitations, and briefly discuss the various relevant data sources.

In-situ networks

In-situ measurements have the advantage of directly measuring the quantities of greatest interest, the variables of state: pressure, temperature, wind, humidity etc. However, at the outset, these fields are rarely sampled on uniform grids; more typically they are sampled on sparse fractal networks (see Fig. 3.6a for an example). In addition, standard geostatistical techniques such as Kriging require various regularity and uniformity assumptions which are unlikely to be satisfied by the data (as we shall see, the latter are more accurately densities of measures which are singular with respect to the usual Lebesgue measures). This means that the results will depend in power law ways on their resolutions.

At first sight, an in-situ measurement might appear to be a "point" measurement, but this is misleading since while their spatial extents may be tiny compared to the analysis grids, what is relevant is rather their *space-time resolutions*, and in practice this is never point-like – nontrivial amounts of either spatial or temporal averaging are required. The main exceptions would be measurements simultaneously near 10 kHz in time and at 0.1–1 mm in space, which would allow one to approach the typical viscous dissipation (and hence true homogeneity) space and time scales.

In-situ measurements: aircraft, sondes

In-situ measurement techniques such as aircraft (horizontal) or sondes (vertical) have other problems, some of which we detail in later chapters. Aircraft data are particularly important. In many

© in this web service Cambridge University Press www.cambridge.org

CAMBRIDGE

Cambridge University Press
978-1-107-01898-3 - The Weather and Climate: Emergent Laws and Multifractal Cascades
Shaun Lovejoy and Daniel Schertzer
Excerpt
More information

cases they provide our only direct measurements of the horizontal statistics. Unfortunately aircraft don't fly in perfectly flat straight trajectories; due to the very turbulence that they attempt to measure, the trajectories turn out to be more nearly fractal and – this turns out to be even more important – their average slopes with respect to the vertical are typically nonnegligible. If one assumes that the turbulence is isotropic (or at least has the same statistical exponents in the horizontal as in the vertical), then this issue is of little importance: if one measures a scaling exponent, then by the isotropy assumption it is unique so that the exponent estimate is assumed to be correct. However, it turns out that if the turbulence is strongly anisotropic, with different exponents in the horizontal and vertical directions, then (as we show in Chapter 6) the interpretation of the measurements is fraught with difficulties and one will generally observe a break in the spectrum/scaling. For the smaller scales the statistics are dominated by the horizontal fluctuations, while at the larger scales they are dominated by the vertical fluctuations. In Chapter 2 we see that naive use of isotropy assumptions has commonly led researchers to misinterpret this spurious transition from horizontal to vertical scaling as a signature of a real physical transition from an isotropic 3D turbulence regime at small scales to an isotropic 2D turbulence regime at large scales.

Remote sensing

One way of overcoming the problems of in-situ sampling is to use remotely sensed radiances. There is a long history of using radiances in "inversion algorithms" in an attempt to directly estimate atmospheric parameters (Rodgers, 1976). However, to be useful in numerical weather models, the data extracted from the inversions must generally be of high accuracy. This is because models typically require gradients of wind, temperature, humidity etc., and taking the gradients greatly amplifies errors. The fundamental problem is that classical inversion techniques aim to estimate the traditional numerical model inputs (variables of state) and they rely on unrealistic subsensor resolution homogeneity assumptions to relate these parameters to the measured radiances. Since the heterogeneity is generally very strong (scaling, multifractal) there are systematic power law dependencies on the resolution of the measurements (a consequence of the cascades structure, Section 5.3). Therefore, new resolution-independent algorithms are needed (Lovejoy *et al.*, 2001).

Reanalyses

Having recognized that in-situ measurements have frequent "holes," and that the inversion of remote measurements is error-prone, one can attempt to combine all the available data as well as the theoretical constraints implied by the governing atmospheric equations to obtain an "optimum estimate" of the state of the atmosphere; these are the meteorological "reanalyses." Reanalyses are effectively attempts to provide the most accurate set of fields consistent with the data and with the numerical dynamical models, themselves believed to embody the relevant physical laws. The data are integrated in space with the help of a variational algorithm either at regular intervals ("3D var"); or – in the more sophisticated "4D var" – both in space and time (see e.g. Kalnay, 2003). In these frameworks, remotely sensed data can also be used, but in a *forward* rather than an inverse model: one simply calculates theoretically the radiances from the guess fields of the traditional atmospheric variables. Once all the guess fields are calculated at the observation times and places, then the two are combined by weighting each guess and measurement pair according to pre-established uncertainties. While these sophisticated data assimilation techniques are elegant, one should not forget that they are predicated on various smoothness and regularity assumptions which are in fact not satisfied because of the very singular scaling effects discussed in this book. These resolution effects introduce nonnegligible uncertainties and possible biases on the reanalyzed fields.

1.2.3 The horizontal scaling of atmospheric fields

We start our tour by considering global-scale satellite radiances, since they are quite straightforward to interpret. Fig. 1.2 shows the "along track" 1D spectra from the Visible Infrared Sounder (VIRS) instrument of the Tropical Rainfall Measurement Mission (TRMM) at wavelengths of 0.630, 1.60, 3.75, 10.8, 12.0 μm, i.e. for visible, near infrared and (the last two) thermal infrared. Each channel was recorded at a nominal resolution of 2.2 km and was scanned over a "swath" 780 km wide, and ≈ 1000 orbits were used in the analysis. The scaling apparently continues from the largest scales (20 000 km) to the smallest available. At scales

© in this web service Cambridge University Press www.cambridge.org

CAMBRIDGE

Cambridge University Press
978-1-107-01898-3 - The Weather and Climate: Emergent Laws and Multifractal Cascades
Shaun Lovejoy and Daniel Schertzer
Excerpt
More information

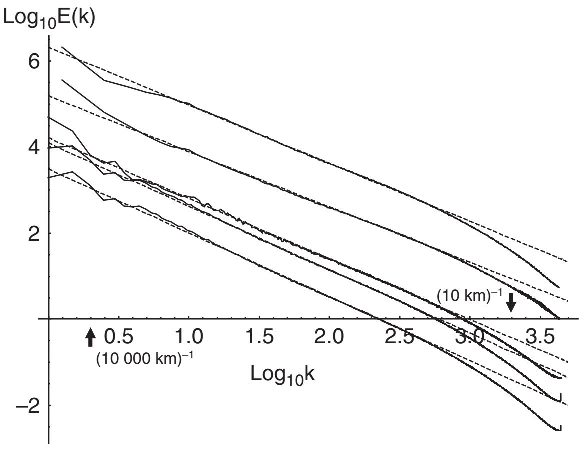

Fig. 1.2 Spectra from ≈ 1000 orbits of the Visible Infrared Sounder (VIRS) instrument on the TRMM satellite channels 1–5 (at wavelengths of 0.630, 1.60, 3.75, 10.8, 12.0 μm from top to bottom, displaced in the vertical for clarity). The data are for the period January through March 1998 and have nominal resolutions of 2.2 km. The straight regression lines have spectral exponents $\beta = 1.35, 1.29, 1.41, 1.47, 1.49$ respectively, close to the value $\beta = 1.53$ corresponding to the spectrum of passive scalars (= 5/3 minus intermittency corrections: see Chapter 3). The units are such that $k = 1$ is the wavenumber corresponding to the size of the planet $(20\ 000\ \text{km})^{-1}$. Channels 1, 2 are reflected solar radiation so that only the 15 600 km sections of orbits with maximum solar radiation were used. The high-wavenumber fall-off is due to the finite resolution of the instruments. To understand the figure we note that the VIRS bands 1, 2 are essentially reflected sunlight (with very little emission and absorption), so that for thin clouds the signal comes from variations in the surface albedo (influenced by the topography and other factors), while for thicker clouds it comes from nearer the cloud top via (multiple) geometric and Mie scattering. As the wavelength increases into the thermal IR, the radiances are increasingly due to black body emission and absorption with very little multiple scattering. Whereas at the visible wavelengths we would expect the signal to be influenced by the statistics of cloud liquid water density, for the thermal IR wavelengths it would rather be dominated by the statistics of temperature variations – themselves also close to those of passive scalars. Adapted from Lovejoy *et al.* (2008).

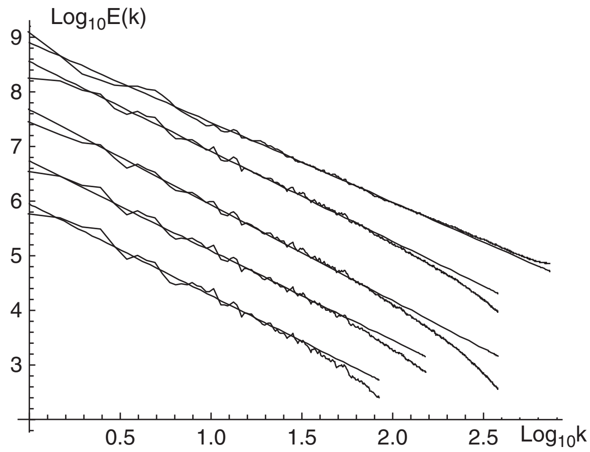

Fig. 1.3 Spectra of radiances from the TRMM Microwave Imager (TMI) from the TRMM satellite, ≈ 1000 orbits from January through March 1998. From bottom to top, the data are from channels 1, 3, 5, 6, 8 (vertical polarizations, 2.8, 1.55, 1.41, 0.81, 0.351 cm) with spectral exponents $\beta = 1.68, 1.65, 1.75, 1.65, 1.46$ respectively at resolutions 117, 65, 26, 26, 13 km (hence the high wavenumber cutoffs), each separated by one order of magnitude for clarity. To understand these thermal microwave results, recall that they have contributions from surface reflectance, water vapour and cloud and rain. Since the particles are smaller than the wavelengths this is the Rayleigh scattering regime and as the wavelength increases from 3.5 mm to 2.8 cm the emissivity/absorbtivity due to cloud and precipitation decreases so that more and more of the signal originates in the lower reaches of clouds and underlying surface. Also, the ratio of scattering to absorption increases with increasing wavelength so that at 2.8 cm multiple scattering can be important in raining regions. The overall result is that the horizontal gradients – which will influence the spectrum – will increasingly reflect large internal liquid water gradients.

below about 10 km, there is a more rapid fall-off but this is likely to be an artefact of the instrument, whose sensitivity starts to drop off at scales a little larger than the nominal resolution. The scaling observed in the visible channel (1) and the thermal IR channels (4, 5) are particularly significant since they are representative respectively of the energy-containing short- and long-wave radiation fields which dominate the earth's energy budget. One sees that thanks to the effects of cloud modulation, the radiances are very accurately scaling. This result is incompatible with classical turbulence cascade models which assume well-defined energy flux sources and sinks with a source and sink-free "inertial" range in between (see Section 2.6.6). Also of interest is the fact that the spectral slope β is close (but a little lower) than the value $\beta = 5/3$ expected for passive scalars in the classical Corrsin–Obukhov theory discussed in Chapter 2. This result is consistent with theoretical studies of radiative transfer through passive scalar clouds (Watson *et al.*, 2009; Lovejoy *et al.*, 2009a). Although we cannot directly interpret the radiance spectra in terms of the wind, humidity or other atmospheric fields, they are strongly nonlinearly coupled to these fields so that the scaling of the radiances are *prima facie* evidence for the scaling of the variables of state. To put it the other way around: if the dynamics were such that it predominantly produced structures at a characteristic scale *L*, then it is hard to see how this scale would not be clearly visible in the associated cloud radiances.

To bolster this interpretation, we can also consider the corresponding images at microwave channels (corresponding to black body thermal emission with wavelengths in the range 0.351–3.0 cm) (Fig. 1.3). In

© in this web service Cambridge University Press www.cambridge.org

Cambridge University Press
978-1-107-01898-3 - The Weather and Climate: Emergent Laws and Multifractal Cascades
Shaun Lovejoy and Daniel Schertzer
Excerpt
More information

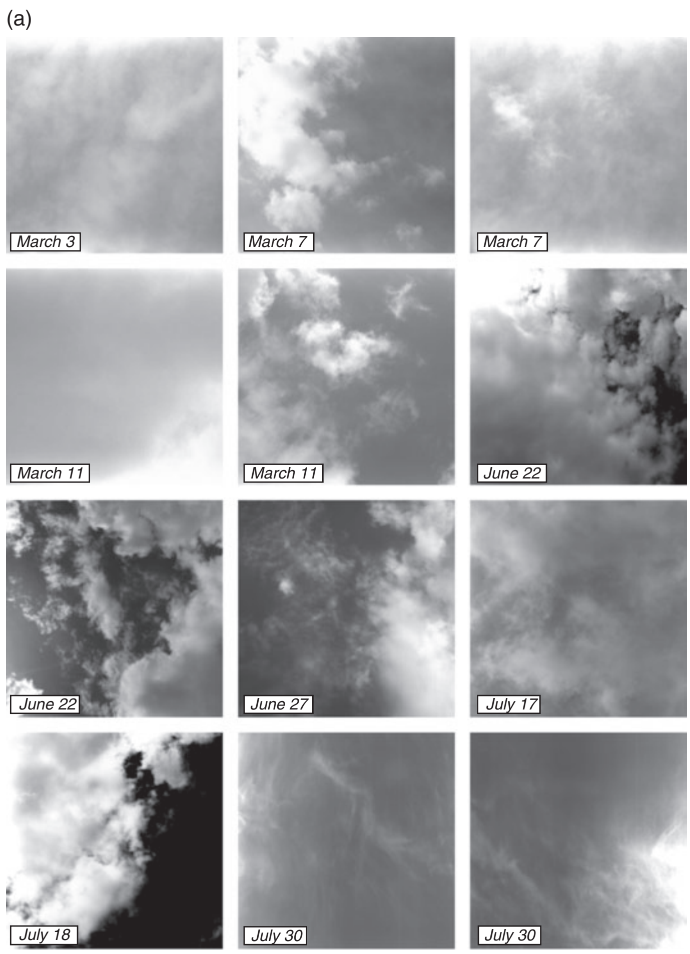

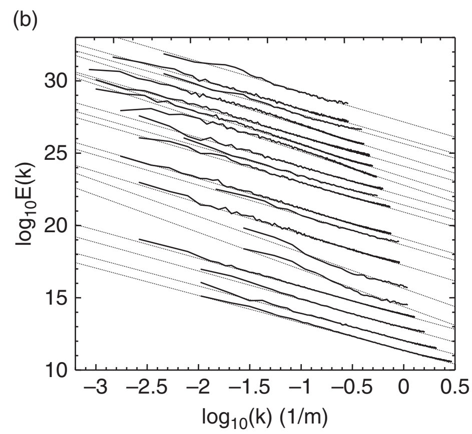

Fig. 1.4 (a) A sample of cloud pictures taken looking upward from the ground near midday, Montreal, Quebec. To get a useful resolution of several thousand pixels on a side, the standard 8 bit imagery of commercial digital cameras is not adequate. In the figure it was necessary to scan black and white negatives (with effectively 13–14 bit dynamical range); the figure shows typical results in the latter case using large-format (60 × 60 mm) negatives to resolutions (for low-lying clouds) down to 50 cm or so. Reproduced from Sachs *et al.* (2002). (b) The spectra of the 19 (of 38) highest-resolution clouds analyzed in with a spectral slope $\beta \approx 2$; see Fig. 1.4a for 12 of the samples. Reproduced from Sachs *et al.* (2002).

order to extend these results to smaller scales, we can use either finer-resolution satellites such MODIS, SPOT or LANDSAT, or we can turn to ground-based photography (Figs. 1.4a, 1.4b). Again, we see no evidence for a scale break. Interestingly, the average exponent $\beta \approx 2$ indicates that the downward radiances captured here (with near-uniform background sky) are smoother (larger β) than for the upward radiances analysed in Figs. 1.2 and 1.3 (the variability falls off more rapidly with wavenumber since β is larger).

The remotely sensed data analyzed above give strong direct evidence of the wide-range scaling of the radiances and hence indirectly for the usual meteorological variables of state. For more direct analyses, we therefore turn our attention to reanalyses. Fig. 1.5a shows representative reanalyses taken from the European Medium Range Weather Forecasting Centre (ECMWF) "interim" reanalysis products, the zonal and meridional wind, the geopotential height, the specific humidity, the temperature, vertical wind. The ECMWF interim reanalyses are the successor products to the ECMWF 40-year reanalysis (ERA40) and are publicly available at 1.5° resolution in the horizontal and at 37 constant pressure surfaces (every 25 mb in the lower atmosphere). At the time of writing, the fields were available every 6 hours from 1989 to the present. The data in Fig. 1.5a were taken from the 700 mb level. The 700 mb level was chosen since it is near the data-rich surface level, but suffers little from the extrapolations necessary to obtain global 1000 mb fields (which is especially problematic in mountainous regions); it gives a better representation of the "free" atmosphere (see Section 4.2.2 for more information and analyses, and Berrisford *et al.*, 2009, for complete reanalysis details).

© in this web service Cambridge University Press

CAMBRIDGE

Cambridge University Press
978-1-107-01898-3 - The Weather and Climate: Emergent Laws and Multifractal Cascades
Shaun Lovejoy and Daniel Schertzer
Excerpt
More information

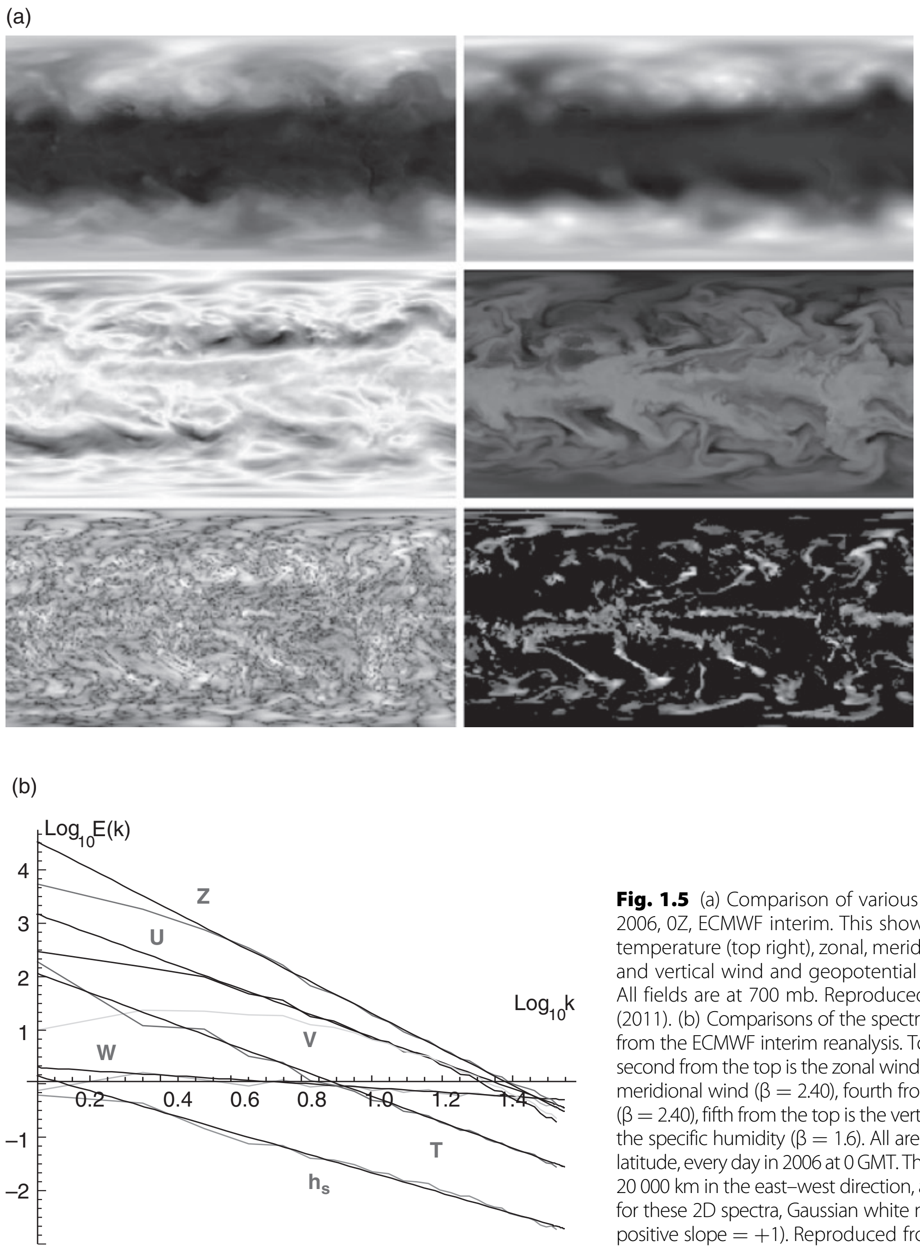

Fig. 1.5 (a) Comparison of various reanalysis fields for January 1 2006, 0Z, ECMWF interim. This shows the specific humidity (top left), temperature (top right), zonal, meridional wind (middle left and right), and vertical wind and geopotential height (bottom left and right). All fields are at 700 mb. Reproduced from Lovejoy and Schertzer (2011). (b) Comparisons of the spectra of different atmospheric fields from the ECMWF interim reanalysis. Top is the geopotential ($\beta = 3.35$), second from the top is the zonal wind ($\beta = 2.40$), third from the top is the meridional wind ($\beta = 2.40$), fourth from the top is the temperature ($\beta = 2.40$), fifth from the top is the vertical wind ($\beta = 0.4$), at the bottom is the specific humidity ($\beta = 1.6$). All are at 700 mb and between $\pm$ 45° latitude, every day in 2006 at 0 GMT. The scale at the far left corresponds to 20 000 km in the east–west direction, at the far right to 660 km. Note that for these 2D spectra, Gaussian white noise would yield $\beta = -1$ (i.e. a positive slope $= +1$). Reproduced from Lovejoy and Schertzer (2011).

The data analyzed were daily data for the year 2006 with only the band between $\pm$ 45° latitude used (with a cylindrical projection). The reason for this choice was twofold: first, this region is fairly data-rich compared to the more extreme latitudes; second, it allows us to conveniently compare the statistics in the east–west and north–south directions in order to study the statistical anisotropies between the two. In addition, the east–west direction was similarly broken up into two sections, one from 0° to 180° and the other from 180° to 0° longitude. For technical reasons (discussed in Chapter 6), the spectrum was estimated by performing integrals around ellipses with aspect ratios 2 : 1 (EW : NS). The wavenumber scale in Fig. 1.5b indicates the east–west scale; a full discussion of the anisotropy is postponed to Chapter 6.

From the figure we can see that the scaling is convincing (with generally only small deviations at the largest scales, $\geq$ 5000 km), although for the

© in this web service Cambridge University Press www.cambridge.org

CAMBRIDGE

Cambridge University Press
978-1-107-01898-3 - The Weather and Climate: Emergent Laws and Multifractal Cascades
Shaun Lovejoy and Daniel Schertzer
Excerpt
More information

geopotential the deviations begin nearer to 2500 km. In spite of this generally excellent scaling, the values of the exponents are not "classical" in the sense that they do not correspond to the values predicted by any accepted turbulence theory. An exception is the value $\beta \approx 1.6$ for the humidity, which is only a bit bigger than the Corrsin–Obukhov passive scalar value 5/3 (minus intermittency corrections, which for this are of the order of 0.15; see Chapter 3), although in any case classical (isotropic) turbulence theory would certainly not be expected to apply at these scales. We could also mention that classically the atmosphere is "thin" at these scales (since the horizontal resolution ≈ 166 km is much greater than the exponential "scale height" ≈ 10 km), and hence according to the classical isotropic 3D/2D theory one would expect 2D isotropic turbulence to apply. For the horizontal wind field this leads to the predictions $\beta = 3$ (a downscale enstrophy cascade) and $\beta = 5/3$ (an upscale energy cascade; see Chapter 2). In comparison, we see that the actual value for the zonal wind ($\beta = 2.35$) is in between the two. In Chapter 6 we argue that this is an artefact of using gradually sloping isobars (rather than isoheights) in a strongly anisotropic (stratified) turbulence. These spectra already caution us that in spite of the intentions of their creators, the reanalyses should not be mistaken for real-world fields. Indeed, it is only by comparing the reanalysis statistics (especially the scaling exponents) with those from other (e.g. aircraft) sources that they can be validated through scale-by-scale statistical comparisons.

Satellite imagery and reanalyses are the only sources of gridded global scale fields, and we have mentioned some of the limitations of each. We therefore now turn our attention to in-situ aircraft data. First consider the 12 m resolution data from an experimental campaign over the Sea of China (Figs. 1.6a, 1.6b). We see that the scaling for both the temperature and horizontal wind is excellent. In both cases, the value $\beta \approx 1.7$ (near the Kolmogorov value 5/3) is reasonable, although in the case of the temperature we have added reference slopes with $\beta = 1.9$, which seems closer to those of the more recent data analyzed in Fig. 1.6c over the larger range 560 m to 1140 km. Once again, the scaling is excellent. We have deliberately postponed discussion of the larger-scale wind field to Chapters 2 and 6, since somewhere between ≈ 30 and 200 km (i.e. a bit beyond the range of Fig. 1.6b) it displays what is

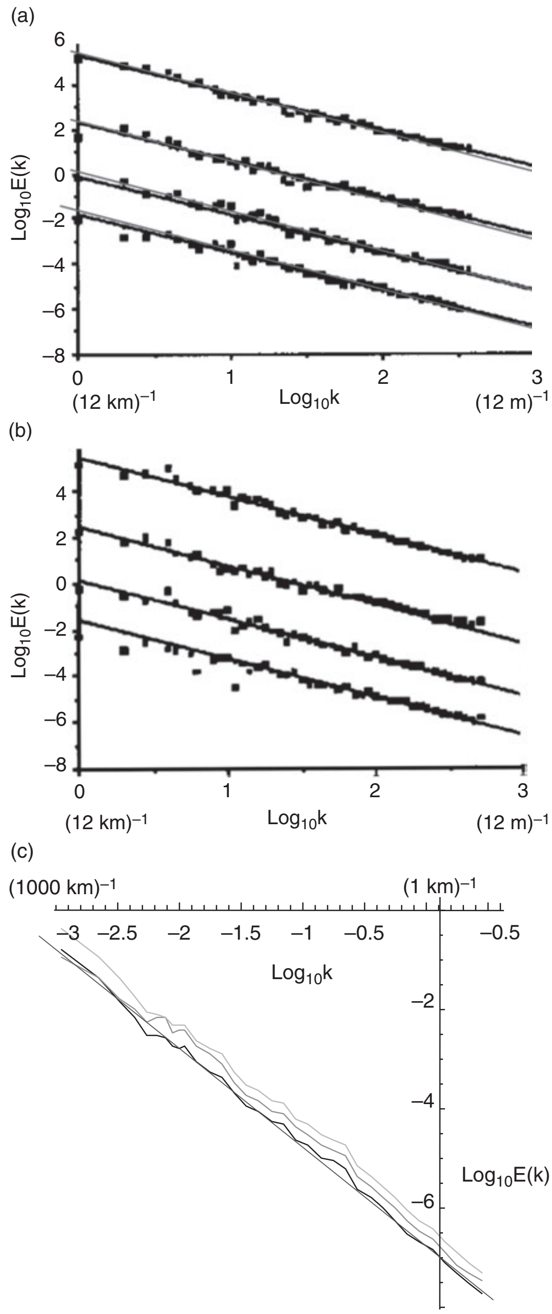

Fig. 1.6 (a) Aircraft temperature spectra. Grey slopes are 1.9, black 1.7. The bottom three curves are averages of 10 samples and each curve is taken at roughly a one-year interval; the top curve is the overall ensemble average. The curves are displaced in the vertical for clarity. Adapted from Chigirinskaya *et al.* (1994). (b) The same as Fig. 1.6a but for the horizontal wind spectrum; slopes of 1.68 are indicated. Adapted from Chigirinskaya *et al.* (1994). (c) Aircraft spectra of temperature (bottom), humidity (middle), log potential temperature (top); reference lines $\beta = 2$. These are averages over 24 isobaric aircraft "legs" near 200 mb taken over the Pacific Ocean during the Pacific Winter Storms 2004 experiment; the resolution was 280 m; Nyquist wavenumber = $(560\ m)^{-1}$. Adapted from Lovejoy *et al.* (2010).

© in this web service Cambridge University Press www.cambridge.org